NASA TECHNICAL NOTE

NASA TN D-2817

NASA TN D-2817

EFFECT OF 40-MEV PROTONS ON SEMICONDUCTORS AS DETERMINED WITH AN IMPROVED METHOD OF MEASURING DIFFUSION LENGTH OF MINORITY CARRIERS

by Marvin E. Beatty and Gerald F. Hill

Langley Research Center
Langley Station, Hampton, Va.

NATIONAL AERONAUTICS AND SPACE ADMINISTRATION • WASHINGTON, D. C. • JUNE 1965

NASA TN D-2817

EFFECT OF 40-MEV PROTONS ON SEMICONDUCTORS AS DETERMINED WITH AN IMPROVED METHOD OF MEASURING DIFFUSION LENGTH OF MINORITY CARRIERS

By Marvin E. Beatty and Gerald F. Hill

Langley Research Center
Langley Station, Hampton, Va.

NATIONAL AERONAUTICS AND SPACE ADMINISTRATION

For sale by the Clearinghouse for Federal Scientific and Technical Information
Springfield, Virginia 22151 – Price $1.00

EFFECT OF 40-MEV PROTONS ON SEMICONDUCTORS AS DETERMINED WITH AN IMPROVED METHOD OF MEASURING DIFFUSION LENGTH OF MINORITY CARRIERS

By Marvin E. Beatty and Gerald F. Hill
Langley Research Center

SUMMARY

Radiation-induced changes in semiconductor materials from 40-MeV protons were observed during irradiation. These changes were determined by the application of an improved infrared method for obtaining the diffusion length of the minority carrier in the semiconductor material. The semiconductor materials investigated comprised the base region of p-n junction photovoltaic devices. The diffusion length and lifetime before, during, and after irradiation are presented in both graphic and tabular form as a function of integrated proton flux. The data obtained show that very short carrier lifetimes may be calculated by employing the infrared method.

Author

INTRODUCTION

Results of recent investigations have shown that the presence of the Van Allen radiation belts, solar flares, and the artificial radiation belt from nuclear bomb testing are detrimental to semiconductor components. The 40-MeV protons used in this investigation are reasonably typical of those found in space. The value of the minority-carrier capture cross section for most semiconductor materials is very high for 40-MeV protons; therefore, 40-MeV protons are especially damaging to the structure of semiconductor materials.

In carrying out research programs to determine mechanisms causing radiation damage to semiconductors, it has been shown that measurement of the lifetime as a function of temperature after irradiation will lead to determination of induced energy levels and minority-carrier capture cross section (refs. 1 and 2). These parameters may be obtained both by the p-n junction method discussed in this report and by methods used in basic material studies, such as electron-spin resonance, Hall effect, and infrared absorption. The values obtained may be combined to help determine the basic damage mechanism from particulate radiation in semiconductor materials and p-n junctions.

The lifetime of minority carriers in a semiconductor material is defined as the average time that excess minority carriers (electrons or holes) will exist before they are reduced to a factor of $1/e$ of their original number because of the recombination process. The lifetime is analogous to a quantity known as the diffusion length, which is defined as the distance moved by the minority carriers before being reduced to a factor of $1/e$ of their original number because of the recombination process. The diffusion of the minority carriers generates the current to be measured. The diffusion length L can be obtained from the lifetime τ, or vice versa, by the relation

$$\tau = \frac{L^2}{D}$$

where D is the diffusion coefficient.

The method of determining τ that was chosen for this investigation is to use an infrared monochromatic light source and measure the diffusion length in the n- and p-type base regions of p-n junction photovoltaic devices (solar cells). This infrared method is more accurate than the direct measurement of τ in photovoltaic devices where excess carriers are produced by a pulsed light source and the decay of photoconductivity is observed on an oscilloscope (ref. 2). With the infrared method, it is possible to minimize surface effects and obtain the lifetime of the particular semiconductor material in the base region of the p-n junction. The infrared method is very sensitive; lifetimes as short as 10^{-10} second can be obtained. The conventional pulsed light technique is limited to lifetimes of approximately 10^{-7} second (ref. 2). A third method has been described which will yield the diffusion length from bombardment of a p-n junction with electrons (ref. 3) but this method is not applicable to proton accelerators because of the low proton flux. The infrared method is applicable to measurement during irradiation by both protons and electrons. In addition, the infrared method is especially useful in investigating gallium arsenide (GaAs) and other semiconductor materials which have very short lifetimes.

This infrared method is especially useful in making measurements with a proton accelerator. The current induced in the cell from a proton accelerator is too low to permit measurement of diffusion length directly as with an electron accelerator. For this reason a technique such as the one described in this report is necessary for proton damage work with solar cells (when determining diffusion length and lifetime). Also, the infrared light source and its associated equipment are portable, and they can be used in the laboratory and at accelerator sites as well.

The 40-MeV proton irradiation was performed with the linear accelerator at the University of Minnesota.

SYMBOLS

A	area, cm^2
C_1, C_2, C_3	constants determined by boundary conditions
D	minority-carrier diffusion coefficient, cm^2/sec
D_b	minority-carrier diffusion coefficient in base layer, cm^2/sec
D_s	minority-carrier diffusion coefficient in surface layer, cm^2/sec
e	base of natural logarithm (2.72)
F_b	flux of minority carriers from base region into space-charge region
H	absolute light energy density, $\mu watts/cm^2$
$h\nu$	photon energy (where h is the Planck constant and ν is the frequency), eV
I	short-circuit current, $\mu amperes$
J_b	flux of minority-carrier charge in base region (short-circuit-current density), $amperes/cm^2$
L	diffusion length of minority carrier, microns
L_b	diffusion length of minority carrier in base region
L_s	diffusion length of minority carrier in surface layer
N_o	incident photon flux density, $photons/cm^2$
q	charge of electron $\left(1.6 \times 10^{-19}\ coulomb\right)$
R	coefficient of reflection for wavelength λ
V_b	surface recombination velocity at base layer surface
X_b	thickness of base layer
X_s	thickness of surface layer
x_b	variable depth in base region
α	absorption coefficient for wavelength λ, cm^{-1}

λ	wavelength, microns
τ	lifetime of minority carrier, sec

Notation

GaAs	gallium arsenide
MeV	million electron volts
n	nano (10^{-9})
n-p	n-type material (surface layer) on p-type material (base)
n-type	material with excess of electrons
p-n	p-type material (surface layer) on n-type material (base)
p-type	material with excess of holes
Si	silicon
SiO	silicon monoxide
μ	micron (10^{-4} cm)

THEORY

In a solar cell, excess electrons and holes are generated by photons incident upon the lattice. These carriers diffuse toward the junction and reach the space-charge region where the minority carriers move across the junction because of the internal field. A decrease in the voltage drop across the junction occurs and a voltage between the contact surfaces is established which can move current through an external circuit. The theoretical expression for the diffusion of the minority carriers as related to the short-circuit current of a solar cell has been determined as a function of incident-light wavelength (refs. 4, 5, and 6). A rigorous derivation of this equation as presented in the appendix yields the following general relation:

$$\frac{1}{L_b} = \alpha\left[\frac{AH(1 - R)}{(h\nu)I} - 1\right]$$

The results of this theoretical expression have been compared with experimental results (refs. 4 and 6).

By using light of a particular wavelength that produces current only in the base region of a solar cell, the diffusion length may be obtained from this

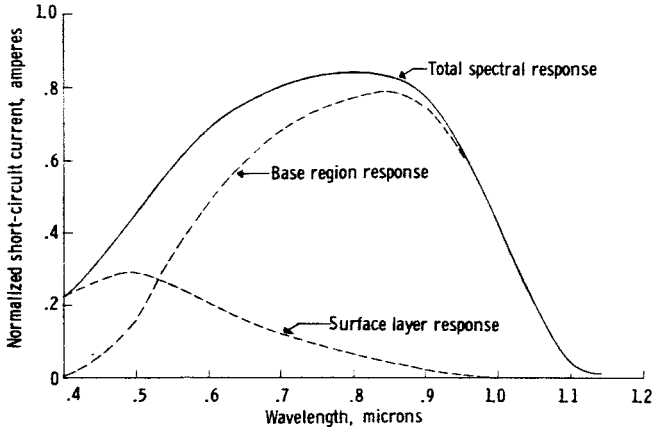

Figure 1.- Theoretical spectral response of silicon solar cell.

relation. Figure 1 (from ref. 5) shows the computed total spectral response of a typical silicon (Si) solar cell, as well as the separate contributions of the surface layer and the base region. It is noted that at wavelengths greater than 0.9μ the surface-layer response is quite small and that most of the current is produced in the base region. In the 40-MeV proton experiment monochromatic light with a wavelength of 1μ was used. The absorption coefficient α for silicon at 1.0μ has been found to be 110 cm^{-1} (ref. 7) and α for gallium arsenide at 1.0μ is approximately 5.0 cm^{-1} (ref. 8).

The phenomenon of wavelength dependence on current generation in a solar cell is more clearly seen in figure 2 where the different phenomena are indicated by the circled numbers (ref. 9):

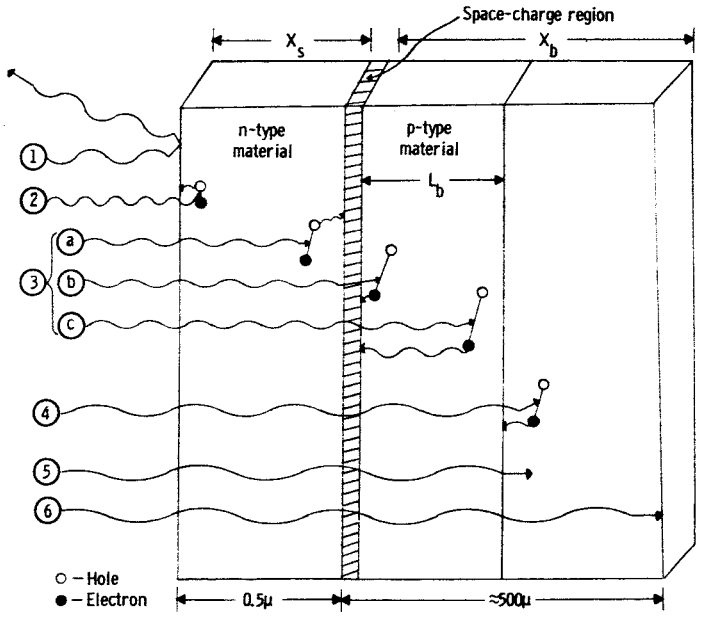

Figure 2.- Illustration of a p-n junction depicting effect of wavelength on production of current.

① A fraction of the incident photons are reflected.

② Photons with very short wavelengths generate many electron-hole pairs very close to the surface but these pairs quickly recombine because of surface recombination. (Little is known about the surface recombination; therefore, it is difficult to observe the surface diffusion length.)

③a Photons with wavelengths in the visible region of the spectrum generate electron-hole pairs which can diffuse to the space-charge region and contribute to the total short-circuit current. But, since a large portion of these pairs are still being formed in the thin surface layer (≈0.5μ thick), there is still a large percentage of pairs being recombined because of the surface recombination velocity.

(3b) Photons with wavelengths in the near infrared generate electron-hole pairs primarily in the base region of the cell which are within a diffusion length of the space-charge region.

(3c) Photons in this part of the spectrum are used to determine measurements of L and τ.

(4) Some pairs are formed outside L and do not contribute to I.

(5) Photons are absorbed but the absorbed energy is insufficient to generate electron-hole pairs.

(6) The far-infrared wavelengths simply pass through the semiconductor material.

Figure 2 is an approximation which applies to most semiconductor materials now used in solar cells and will vary slightly for the different materials depending on wavelength. The variation of wavelength is mainly due to the photon energy required for creation of electron-hole pairs.

Atomic displacement production is the main source of degradation due to irradiation in the bulk material (refs. 10 and 11). This damage is in the form of vacancy-interstitial atoms which result from an atom being displaced from its normal lattice position by incident radiation. The primary effect of the radiation damage is the introduction of new recombination centers in the base region which reduce carrier lifetime. A corresponding decrease in the diffusion length occurs; therefore, fewer minority carriers reach the junction and the short-circuit current is reduced.

APPARATUS

The apparatus used to measure diffusion length is shown in figure 3. The infrared light source is constructed in four sections, each made of 1/8-inch-thick aluminum to minimize radiation darkening of optical components. Section (1) (fig. 3) houses the lamp and is provided with a fan for cooling. The lamp used in the experiment was a commercial tungsten photospot lamp. Sections (2), (3), and (4) house the lenses and filters. These sections are circular tubing 4 inches in diameter and 1 foot long. The sections are threaded and allow several combinations to be used according to length desired (from 2 to 4 ft) or intensity of light desired on the solar cells. These combinations are beneficial in that the variation allows a certain amount of maneuverability in cramped quarters. The part labeled (5) is an example of a brass holder used to hold a lens and filter in position inside the tubing. The holder is trimmed with heavy felt held by aluminum strips to prevent leakage of light. The two sample holders (designated (6)) are bronze with 1/4-inch copper tubing attached to permit water-cooling. One holder positions cells normal to the light; the other, at an angle of 45°. Terminals are provided for reading I of the samples.

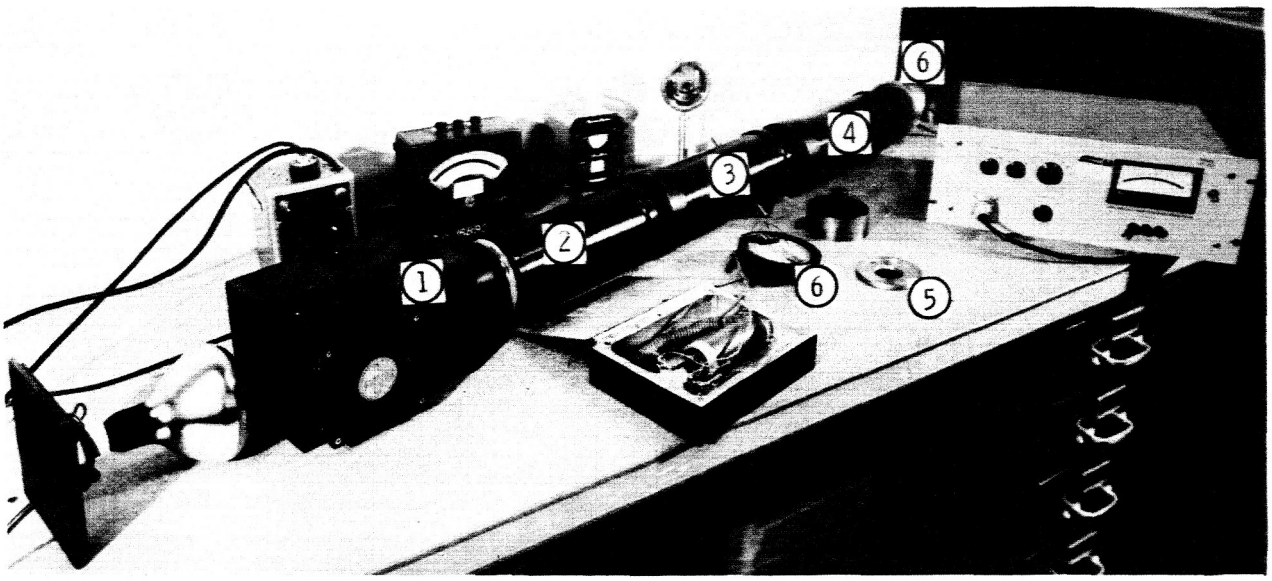

Figure 3.- Apparatus for determination of diffusion length of photovoltaic devices during irradiation. L-64-541.1

The optical lenses enclosed in the tubing of the infrared light source collimate the light. The light beam was approximately 4 inches in diameter and was found to be sufficiently uniform throughout the investigation.

An infrared narrow-band interference filter with a nominal peak transmission of 36 percent at 1.0μ is provided. Transmission through the filter was measured on spectrophotometers having a range of 0.3μ to 16.0μ. It was found that the half-band width was approximately 0.025μ, and that the total transmission outside the transmission band was less than 0.10 percent. This infrared filter may be removed and the system used as a source of white light.

The infrared light source is connected to a voltage regulator to operate the tungsten lamp at various color temperatures, depending on the particular point of interest of the research project. A constant-voltage transformer is connected between the main power supply and the voltage regulator in order to keep a constant voltage at the lamp. The lamp voltage is monitored with a voltmeter. A milli-micro voltmeter is used to read the voltage drop across a precision 0.1-ohm resistor connected in series with the solar cells. A thermopile measured the photon flux passing through the narrow-band filter and incident on the samples. With this setup the short-circuit current generated by the 1μ wavelength illumination is obtained from a photovoltaic device.

40-MEV PROTON EXPERIMENT

The source of the protons used in the 40-MeV proton experiment was the linear accelerator at the University of Minnesota. This accelerator is capable of producing a time-averaged beam current of 10^{-8} ampere (approximately 6×10^{10} protons/sec).

The cross-sectional area of the proton beam was approximately 1.25 sq in. This area was determined by exposure of photographic film to the proton beam. This exposure also established the proper sample position.

An ion chamber was used to monitor the beam and was calibrated against a Faraday cup by using a current integrator. The windows of the chamber were very thin sheets of aluminized plastic film which caused negligible loss to the energy of the proton beam.

The experimental setup used during irradiation is shown in figure 4 and a block diagram of the complete inbeam circuit is shown in figure 5. The previously described apparatus was used. The sample holder angled 45° was used to measure I during pre- and post-irradiation tests. The proton beam was perpendicular to the cells whereas the light was angled approximately 45° from normal during irradiation. A light intensity of approximately $100 \mu watts/cm^2$ was used to generate I. This flux is low enough to prohibit τ from becoming a function of the majority-carrier concentration. A 3-cm water filter was used to reduce the light flux to this low level.

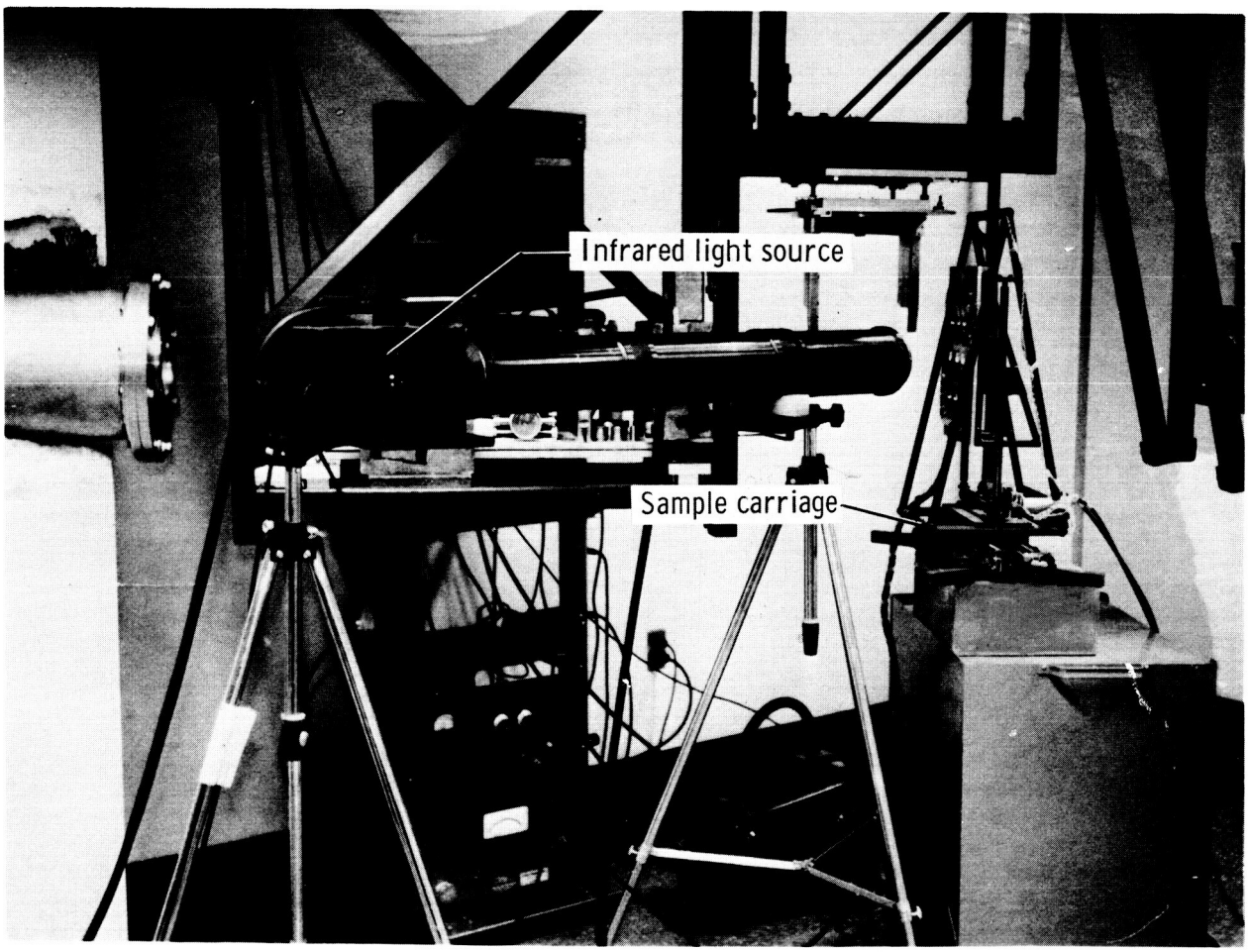

Figure 4.- Typical inbeam setup for determining radiation-induced changes in diffusion length of semiconductors. L-65-49

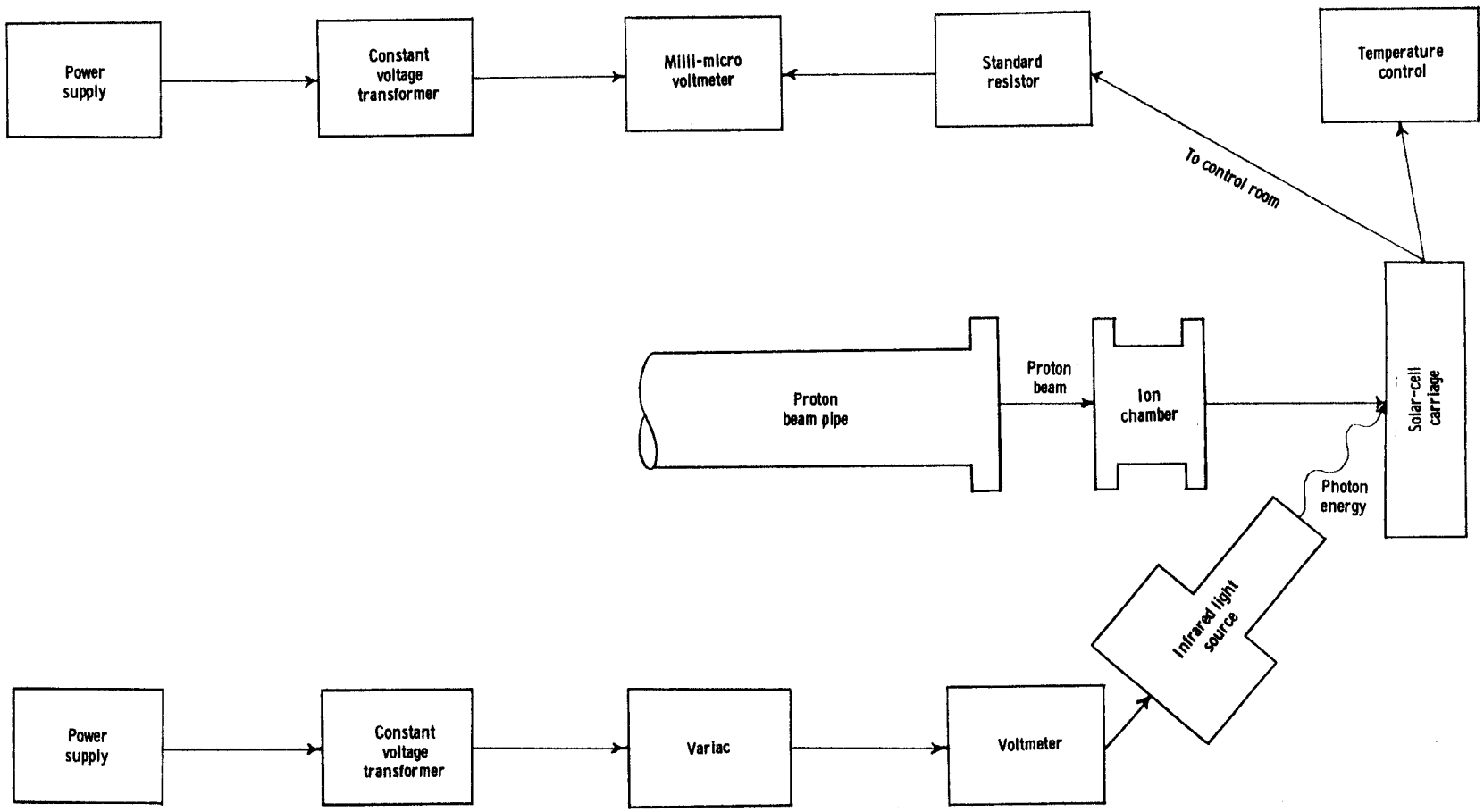

Figure 5.- Block diagram of readout system used in inbeam measurements.

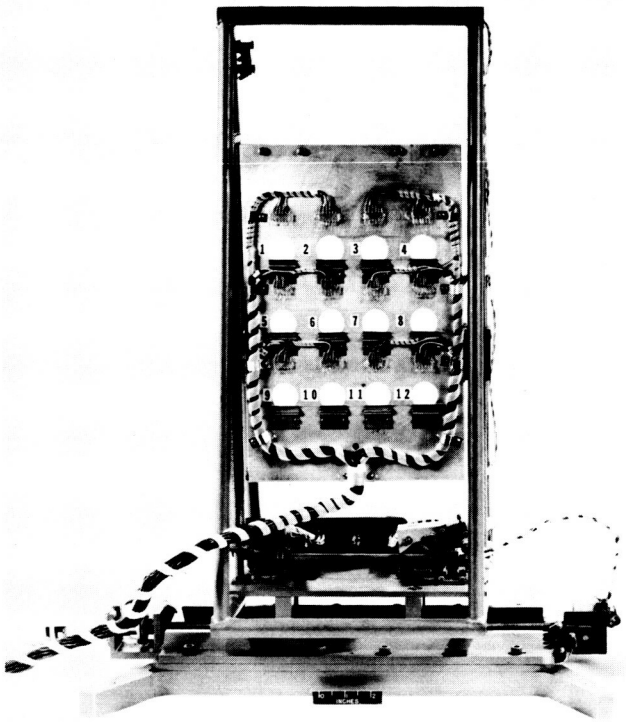

Figure 6.- Sample carriage. L-64-676

The solar cells were mounted on thin ceramic plates with a silicon rubber adhesive for ease in handling. Leads were insulated with teflon for future high-temperature studies. During irradiation, the solar cells were mounted on a carriage (fig. 6) which was designed to move both vertically and horizontally. The carriage was positioned by remote control and monitored with a television camera.

The short-circuit current and photon flux were measured before and after irradiation and periodically during irradiation. In order to obtain accurate results, the room was fully darkened so that the light was from the infrared source alone. Careful experimental techniques were used and very little background effect was noticed.

Because of transient effects from ionization, the short-circuit current is slightly high during radiation incident upon the solar cell. For this reason the beam was momentarily stopped at desired points while readings were made.

The temperature of the samples was maintained at 28° C, ±2° C, and was monitored by a potentiometer-type pyrometer.

After irradiation, the samples were maintained in dry ice to prevent room-temperature annealing, and post-irradiation measurements were carefully checked several days later.

Nine 1- by 2-cm commercial solar cells were irradiated during the 40 MeV test to obtain preliminary results with the test apparatus. Eight of the cells were silicon with SiO antireflectance coatings. These cells were shallow diffused (approximately 1/2μ). The efficiency of these cells varied from 9 to 12 percent. Four of the eight cells were 1- to 2-ohm-cm arsenic doped p-n silicon, with boron diffused surface layer. Four were boron doped n-p silicon, with phosphorous-diffused surface layer having the same resistivity as the p-n samples. One 7.5-percent zinc doped gallium arsenide p-n sample with resistivity 0.2 to 2.0-ohm-cm was also irradiated.

RESULTS

The infrared method used to investigate the diffusion length gave very good repetition of results. Several tests were performed in which typical cells were measured at random intervals with the voltage on the lamp being

varied and the calculated value of L always being repeated within ±5 percent. Pre- and post-irradiation measurements made at the proton accelerator site and Langley Research Center also agreed within ±5 percent.

The data obtained for L and τ are shown in table I. Figures 7 and 8 give the diffusion length and the lifetime, respectively, as a function of integrated proton flux for 40-MeV protons. The data obtained for irradiated n-p and p-n solar cells indicate that the damage to p-type Si is much less than

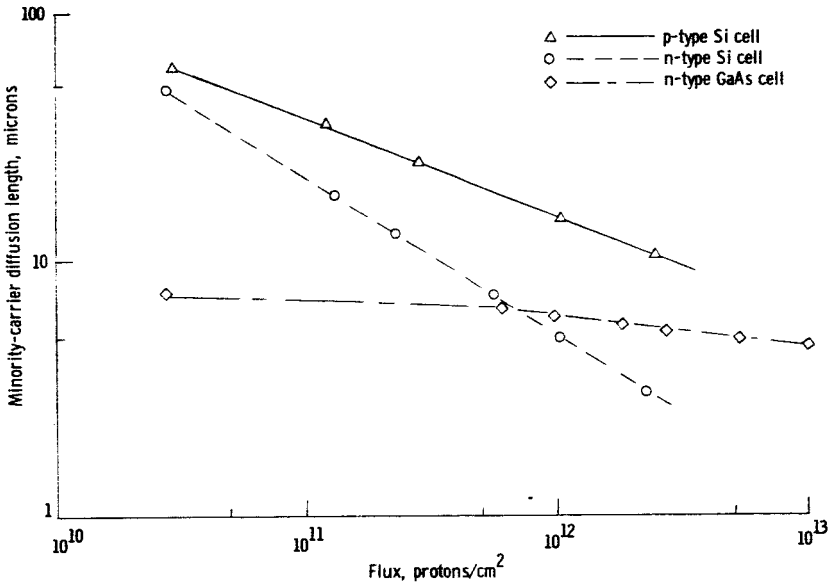

Figure 7.- Minority-carrier diffusion length as a function of total integrated proton flux for typical samples.

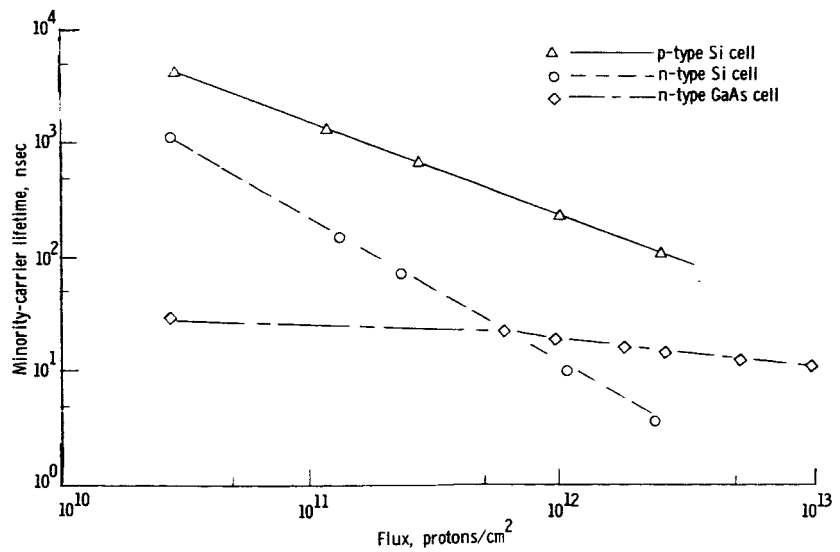

Figure 8.- Minority-carrier lifetime as a function of total integrated proton flux for typical samples.

that to n-type. This lesser damage in p-type Si is believed to be due, in part, to the higher mobility of minority carriers and to a lower minority-carrier capture cross section resulting from the nature of defects produced. The n-type GaAs exhibits less change from radiation damage than either Si type; however, L was initially much lower for n-type GaAs. The data on the GaAs cell also showed that the infrared method was capable of measuring very short values of τ, and that radiation damage to GaAs solar cells should be more thoroughly investigated.

The slopes of the L and τ curves are similar to those from other experiments (refs. 6, 12, and 13). At a total integrated flux of approximately 10^{12} protons/cm^2, L for n-type Si was reduced to a negligible value whereas L for p-type Si was reduced to about 10μ as compared with an initial average L of approximately 50μ for p-type Si. Measurements of L on another manufacturer's cells not irradiated showed a value for L between 90μ and 130μ. The difference is believed to be due to resistivity of the material used and to manufacturing techniques. The diffusion length of n-type GaAs changed by only a few microns as can be seen by figure 7. Irradiation of GaAs at a total integrated flux of 5×10^{13} protons/cm^2 was a heavier dose than that for Si.

The reflection coefficient R of the cells was measured before and after irradiation. The initial values were between 5 and 20 percent, and no change due to radiation was found.

CONCLUDING REMARKS

Radiation-induced changes in semiconductor materials from 40-MeV protons were observed during irradiation. These changes were determined by the application of an improved infrared method for obtaining the diffusion length of the minority carrier in the semiconductor material. The semiconductor materials investigated comprised the base region of p-n junction photovoltaic devices.

A distinct advantage of p-type over n-type Si is shown in regard to damage from 40-MeV-proton radiation; however, n-type gallium arsenide (GaAs) shows even less damage than p-type silicon (Si) when percent of degradation from the initial state is considered. Even though commercial GaAs solar cells are less efficient in current production than Si cells, it is believed that this material demands much investigation as to its possibilities.

The results from measurements of lifetimes and diffusion lengths in solar cells made with the infrared light source are more informative than those of conventional methods because complicated surface effects are reduced to a minimum. This reduction in surface effects allows better accuracy for very short lifetimes. As can be seen from the data, lifetimes as short as 10^{-10} second were determined. This accuracy is very beneficial in investigating the radiation-induced energy levels and minority-carrier capture cross sections in materials with very short initial lifetimes.

The infrared method is especially useful in making measurements with a proton accelerator. The current induced in the cell from a proton accelerator is too low to permit measurement of diffusion length directly as with an electron accelerator. For this reason a technique such as the one described in this report is necessary for proton damage work with solar cells (when determining diffusion length and lifetime). Also, the infrared light source and its associated equipment are portable, and they can be used in the laboratory and at accelerator sites as well.

Finally, the determination of the radiation-induced energy levels and capture cross section determined from measurements of lifetime as a function of temperature with the infrared source may be correlated with values obtained from other methods. Methods used in the basic material field include electron-spin resonance, Hall effect, and infrared absorption. A correlation of data gives a better insight into the radiation damage mechanism.

Langley Research Center,
National Aeronautics and Space Administration,
Langley Station, Hampton, Va., February 9, 1965.

APPENDIX A

DERIVATION OF BASE DIFFUSION LENGTH

The derivation of the relation showing the dependence of the short-circuit current on wavelength in a solar cell is given in reference 5. The relationship for the base region of a p-n junction in terms of the general diffusion equation is as follows:

$$\frac{d^2C_2}{dx_b^2} - \frac{C_2}{L_b^2} = -\frac{\alpha N_o(1 - R)}{D_b} e^{-\alpha x_b} \tag{A1}$$

where $N_o(1 - R)$ is the incident photon flux which penetrates the surface. The solution of equation (A1) for $\alpha L_b \neq 1$ is

$$C_2 = C_1 e^{\frac{x_b}{L_b}} + C_3 e^{-\frac{x_b}{L_b}} - \frac{\frac{N_o(1 - R)e^{-\alpha X_s}}{\alpha D_b}}{1 - \frac{1}{\alpha^2 L_b^2}} e^{-\alpha x_b} \tag{A2}$$

The constants C_1 and C_3 are found by applying boundary conditions:

$$C_1 = 0 \qquad x_b = 0 \tag{A3}$$

and

$$\frac{dC_2}{dx_b} = -\frac{V_b}{D_b} C_2 \qquad x_b = X_b \tag{A4}$$

The minority-carrier flux at the edge of the space-charge region is

$$F_b = -D_b \left.\frac{dC_2}{dx_b}\right|_{x_b=0} \tag{A5}$$

The concentration of the minority carrier is zero at the edge of the space-charge region but the flux is not.

The flux of the minority carrier in the base region (short-circuit-current density) is defined by

$$J_b = qF_b \tag{A6}$$

The results of the preceding equation for $\alpha L_b \neq 1$

$$J_b = \frac{qN_o(1 - R)e^{-\alpha X_s}}{1 - \frac{1}{\alpha^2 L_b^2}} \left\{ \frac{1}{\alpha L_b} \left[\frac{V_b \cosh \frac{X_b}{L_b} + \frac{D_b}{L_b} \sinh \frac{X_b}{L_b} - \left(V_b - \alpha D_b\right)e^{-\alpha X_b}}{V_b \sinh \frac{X_b}{L_b} + \frac{D_b}{L_b} \cosh \frac{X_b}{L_b}} \right] - 1 \right\} \tag{A7}$$

where, for commercial cells

$$\frac{X_b}{L_b} \ggg 1 \tag{A8}$$

For a large ratio of thickness to diffusion length, the short-circuit-current density is insensitive to both thickness and surface recombination velocity. By using this large ratio, equation (A7) reduces to

$$J_b = \frac{qN_o(1 - R)e^{-\alpha X_s}}{\frac{\alpha^2 L_b^2 - 1}{\alpha^2 L_b^2}} \left\{ \frac{1}{\alpha L_b} [1] - 1 \right\} \tag{A9}$$

or

$$J_b = \frac{-qN_o(1 - R)\alpha L_b e^{-\alpha X_s}}{1 + \alpha L_b} \tag{A10}$$

Since

$$J_b = \frac{I}{A} \tag{A11}$$

then the absolute magnitude of the current is

$$I = AqN_o(1 - R)\frac{\alpha L_b e^{-\alpha X_s}}{1 + \alpha L_b} \tag{A12}$$

For various wavelengths λ, a different dependence of I on L_b and L_s is found (see figs. 1 and 2):

(1) For long wavelengths ($\lambda \geqq 0.9\mu$), the short-circuit current is primarily proportional to the base diffusion length. These wavelengths are deeply penetrating and excess holes and electrons are released in the base region of the cell. A much smaller number have been released in the surface or skin region.

(2) For short wavelengths ($\lambda < 0.9\mu$), more dependence on current carriers is generated in the surface layer, because these wavelengths are not deeply penetrating and have a smaller effect in the base region than in the skin region. Since many complications arise due to semiconductor surface effects in the skin region, it is very difficult to obtain a reasonable determination of the skin diffusion length (ref. 2).

At longer wavelengths and for commercial cells, the exponential term in equation (A13) may be neglected, since the junction depth is on the order of 1μ or less. The equation now becomes

$$I = AqN_O(1 - R)\frac{\alpha L_b}{1 + \alpha L_b} \tag{A13}$$

Since

$$N_O = \frac{H}{q(h\nu)} \tag{A14}$$

the relationship for the diffusion length becomes

$$\frac{1}{L_b} = \alpha\left[\frac{AH(1 - R)}{(h\nu)I} - 1\right] \tag{A15}$$

REFERENCES

1. Aukerman, L. W.; and Reid, F. J.: Energy Levels Produced in Semiconductors by High-Energy Radiation. Tech. Mem. No. 4, Radiation Effects Inform. Center, Battelle Mem. Inst., July 15, 1958.

2. Loferski, J. J.; and Rappaport, P.: Radiation Damage in Ge and Si Detected by Carrier Lifetime Changes: Damage Thresholds. Phys. Rev., Second ser., vol. 111, no. 2, July 15, 1958, pp. 432-439.

3. Rosenzweig, W.: Diffusion Length Measurement by Means of Ionizing Radiation. Bell System Tech. J., vol. XLI, no. 5, Sept. 1962, pp. 1573-1588.

4. Cummerow, Robert L.: Photovoltaic Effect in p-n Junctions. Phys. Rev., vol. 95, no. 1, July 1, 1954, pp. 16-21.

5. Oliver, J. W.: Charged Particle Radiation Damage in Semiconductors, II: Minority Carrier Diffusion Analysis in Photovoltaic Devices. MR-16 (8987-0001-RU-001), Space Technol. Lab., Inc., Feb. 19, 1962.

6. Bilinski, J. R.; Brooks, E. H.; Cocca, U.; and Maier, R. J.: Proton-Neutron Damage Equivalence in Si and Ge Semiconductors. IEEE, Trans. Nucl. Sci., vol. NS-10, no. 5, Nov. 1963, pp. 71-86.

7. Dash, W. C.; and Newman, R.: Intrinsic Optical Absorption in Single-Crystal Germanium and Silicon at 77°K and 300°K. Phys. Rev., Second ser., vol. 99, no. 4, Aug. 15, 1955, pp. 1151-1155.

8. Sturge, M. D.: Optical Absorption of Gallium Arsenide between 0.6 and 2.75 eV. Phys. Rev. Second ser., vol. 127, no. 3, Aug. 1, 1962, pp. 768-773.

9. Smith, K. D.; Gummel, H. K.; Bode, J. D.; Cuttriss, D. B.; Nielsen, R. J.; and Rosenzweig, W.: The Solar Cells and Their Mounting. Bell System Tech. J., vol. XLII, no. 4, pt. 3, July 1963, pp. 1765-1816.

10. Billington, Douglas S.; and Crawford, James H., Jr.: Radiation Damage in Solids. Princeton Univ. Press, 1961, pp. 57 and 312-368.

11. Seitz, Frederick; and Koehler, J. S.: Displacement of Atoms During Irradiation. Solid State Physics, Vol. 2, Frederick Seitz and David Turnbull, eds., Academic Press, Inc. (New York), 1956, pp. 305-448.

12. Gremmelmaier, R.: Irradiation of P-N Junctions with Gamma Rays: A Method for Measuring Diffusion Lengths. Proc. IRE, vol. 46, no. 6, June 1958, pp. 1045-1049.

13. Loferski, J. J.; and Rappaport, P.: The Effect of Radiation on Silicon Solar-Energy Converters. RCA Rev., vol. XIX, no. 4, Dec. 1958, pp. 536-554.

TABLE I.- PRETEST AND TEST DATA ON SOLAR CELLS IRRADIATED WITH 40-MEV PROTONS

Solar cell	Total flux, protons/cm^2	Short-circuit current, I, μamperes	Diffusion length, L, microns	Lifetime, τ, nsec
n-type GaAs	0	0.23	8.03	32.24
	5.72×10^{11}	.21	7.33	26.86
	9.68	.20	6.98	24.36
	18.5	.19	6.63	21.97
	27.7	.18	6.28	19.72
	39.8	.18	6.28	19.72
	49.1	.17	5.93	17.58
	71.5	.17	5.93	17.58
	93.9	.17	5.93	17.58
	201.6	.16	5.58	15.57
	314.3	.16	5.58	15.57
	534.3	.16	5.58	15.57
p-type Si	0	60	53.43	2850
	1.38×10^{11}	42	31.79	1010
	2.62	35	25.03	630
	3.85	33	23.24	540
	6.05	27	18.17	330
	8.25	24	15.80	250
	10.45	22	14.27	200
	12.65	20	12.79	160
	14.85	19	12.07	150
	17.05	18	11.35	130
	19.25	17	10.65	110
	21.45	16	9.95	100
	23.65	16	9.95	100
n-type Si	0	60	50.79	1032.0
	1.34×10^{11}	28	18.26	133.0
	2.42	22	13.75	73.0
	3.39	18	10.95	48.0
	4.40	15	8.95	32.0
	5.41	13	7.65	23.4
	6.64	11	6.39	16.3
	7.90	10	5.77	13.4
	8.80	8	4.56	8.3
	10.00	7	3.97	6.3
	10.84	6	3.38	4.6
	11.99	5	2.80	3.1
	14.25	4	2.23	2.0
	16.50	2	1.10	.5
	20.98	2	1.10	.5
n-type Si	0	58	47.81	914.0
	$.55 \times 10^{11}$	28	18.14	132.0
	1.51	17	10.21	42.0
	2.31	12	6.98	19.4
	3.06	10	5.74	13.2
	3.98	8	4.54	8.2
	4.66	7	3.95	6.2
	5.81	4	2.21	2.0
	8.01	3	1.65	1.1
	10.20	1	.54	.1
p-type Si	0	42	31.56	1000
	$.97 \times 10^{11}$	32	22.21	490
	1.87	31	21.35	460
	3.26	28	18.86	360
	4.44	26	17.25	300
	5.90	24	15.70	250
	8.10	23	14.93	220
	10.29	20	12.71	160
	13.15	19	11.99	140
	19.75	17	10.58	110
	26.42	16	9.90	100
	33.06	15	9.22	90

TABLE I.- PRETEST AND TEST DATA ON SOLAR CELLS IRRADIATED WITH 40-MEV PROTONS - Concluded

Solar cell	Total flux, protons/cm^2	Short-circuit current, I, μamperes	Diffusion length, L, microns	Lifetime, τ, nsec
n-type Si	0	54	48.18	929.0
	$.68 \times 10^{11}$	27	19.04	104.0
	1.69	17	11.12	49.5
	2.62	11	6.90	19.0
	3.81	8	4.92	9.7
	4.93	6	3.64	5.3
	5.94	4	2.39	2.3
	6.86	4	2.39	2.3
p-type Si	0	56	49.65	2500
	1.01×10^{11}	34	24.81	620
	3.04	26	17.83	320
	3.75	26	17.83	320
	5.06	24	16.21	260
	6.45	22	14.64	210
	8.65	21	13.88	190
	10.84	20	13.12	170
	13.15	20	13.12	170
	15.35	19	12.37	150
	19.75	17	10.91	120
	21.95	17	10.91	120
	28.55	15	9.50	90
	35.15	14	8.81	80
	46.24	12	7.44	60
n-type Si	0	58	56.96	1298.0
	$.506 \times 10^{11}$	22	15.55	96.7
	1.34	14	9.32	34.8
	1.98	12	7.87	24.8
	2.77	11	7.17	20.6
	3.59	6	3.77	5.7
	4.66	5	3.12	3.9
	5.68	4	2.48	2.5
	6.91	2	1.22	.6
	8.32	1	.61	.15
p-type Si	0	56	46.81	2190
	$.66 \times 10^{11}$	38	27.25	740
	1.71	31	21.07	440
	2.78	27	17.82	320
	3.75	26	17.03	290
	4.61	24	15.50	240
	6.81	22	14.01	200
	9.01	21	13.28	180
	11.20	20	12.56	160
	13.40	19	11.85	140
	15.60	19	11.85	140